Perturbation Theory and Sediment Carrying Capacity of Suspended Load in a Tidal River

Qiancheng Xie[1*], James Yang[2, 3], T. Staffan Lundström[1]

1 Fluid and Experimental Mechanics, Luleå University of Technology, Luleå, 97754, Sweden
2 Concrete Structures, Royal Institute of Technology, Stockholm, 10044, Sweden
3 Vattenfall AB, R&D Hydraulic Laboratory, Älvkarleby, 81426, Sweden
* Corresponding author's e-mail: qiancheng.xie@ltu.se

Abstract

In a fluvial river, coastal tides often carry suspended load that dominates the sediment transport. The sediment carrying capacity (SCC) is the amount of suspended load transported by the flow, reflecting the erosion and deposition equilibrium in the water body. Based on the perturbation theory, the study modifies the method for the SCC determination and applies it to a natural river where tidal currents are predominant. In terms of flow velocity, water depth, particle settling velocity, median grain size and tidal range, an approach is established by means of dimensional analysis and multivariate linear regression. Field data are collected to determine and validate coefficients of the SCC formula. Compared to the previous studies with fewer parameters for the correlation analysis, the procedure is an improvement and can be used to estimate the SCC in similar situations.

Keywords: Sediment carrying capacity; Tidal river; Perturbation theory; Suspended load; Field measurements.

1 Introduction

The sediment carrying capacity (SCC) is an index characterizing the interplay between the flow and sediment transport in a river. It is often used for making predictions of the river bedform evolution. During the past decades, many studies have been dedicated to the SCC estimations, leading to numerous theoretical and empirical formulas that contribute to the understanding of the issue (Zhang 1961; Engelund and Hansen 1967). For suspended load, most of the formulas involve four factors i.e., average flow velocity, average water depth, median grain size and particle settling velocity (Milhous 2005; Yang et al. 2007). Affected by river bathymetry, flow and sediment features, the formulas differ in the way of combination of these contributing factors, which is natural. During the recent years, the SCC approach has been extended to the research in estuaries and coastal areas. In a tidal environment, it is not straightforward to make estimations due to the flow complexity, involving the river run-off and tidal currents at different spatial and temporal scales. Hence, the effect of tides including the periodic feature should also be included in the SCC predictions.

The perturbation theory refers to the mathematical tool to obtain an approximate solution to a complex system. It starts with a simplified form of the original problem, simple enough to be solved analytically. A feature of the approach is, by means of dimensionless analysis, to break down the problem into several perturbation parts. The theory is widely used in fluid mechanics and other physical disciplines.

Based on the perturbation theory, the study considers seven major factors and derives a modified SCC formula. Its coefficients are obtained through multivariate linear regression analysis. Field data from a wet and dry season of a typical tidal river are collected to establish and verify the formula. The procedure provides reference for determination of suspended sediment transport in similar situations.

2 Methodology description

For suspended load transport in a tidal river, the SCC, denoted by S_c, is affected by several factors.

$$S_c = f\,(U, h, g, \upsilon, \gamma_s, \gamma, \omega, D_{50}, B, \Delta h, \tilde{h}) \tag{1}$$

where U (m/s) = flow velocity, h (m) = water depth, g (m/s^2) = gravity acceleration, υ (m^2/s) = water viscosity, γ_s (N/m^3) = volumetric mass density of suspended load, γ (N/m^3) = water density, ω (mm/s) = particle settling velocity, D_{50} (mm) = median grain size, B (m) = river width, Δh (m) = water-level difference between two adjacent instants (usually one-hour interval), and $\tilde{h}$ (m) = tidal range, i.e. the difference between the high and low tides within a tidal period. The flow parameters U, h, B, Δh and $\tilde{h}$ refer to the cross-sectionally averaged values.

By dimensionless analysis, Eq. (1) is rewritten as:

$$S_c = f\,(\frac{U^2}{gh}, \frac{D_{50}}{h}, \frac{U}{\omega}, \frac{\gamma_s-\gamma}{\gamma}, \frac{h}{B}, \frac{Uh}{\upsilon}, \frac{\Delta h}{\tilde{h}}) \tag{2}$$

Term $(\gamma_s-\gamma)/\gamma$ is considered as a constant. If the river is wide and the water is shallow, the h/B ratio becomes small and is therefore neglected. The Reynolds effect, $\mathsf{R} = Uh/\upsilon$ is also excluded for flows in a natural river. Eq. (2) thus becomes

$$S_c = f\,(\frac{U^2}{gh}, \frac{D_{50}}{h}, \frac{U}{\omega}, \frac{\Delta h}{\tilde{h}}) \tag{3}$$

In light of the perturbation theory, the contrast relations between flow turbulence intensity ($U^2/(gh)$), relative roughness (D_{50}/h), gravity action (U/ω) and tidal effect ($\Delta h/\tilde{h}$) are written as

$$S_{c1} = S_1 + k_1 \frac{U^2 D_{50}}{gh^2} + k_1^2 \frac{U^2 D_{50}}{gh^2} + k_1^3 \frac{U^2 D_{50}}{gh^2} + \ldots \tag{4}$$

$$S_{c2} = S_2 + k_2 \frac{U^3}{gh\omega} + k_2^2 \frac{U^3}{gh\omega} + k_2^3 \frac{U^3}{gh\omega} + \ldots \tag{5}$$

$$S_{c3} = S_3 + k_3 \frac{U^2 \Delta h}{gh\tilde{h}} + k_3^2 \frac{U^2 \Delta h}{gh\tilde{h}} + k_3^3 \frac{U^2 \Delta h}{gh\tilde{h}} + \ldots \tag{6}$$

where S_1, S_2 and S_3 = constants and k_1, k_2 and k_3 = infinitesimal perturbation variables. The second- and higher-order terms are neglected. Introducing the above expressions into Equation (3) leads to:

$$S_c = S_{c1} + S_{c2} + S_{c3} = S_1 + S_2 + S_3 + k_1 \frac{U^2 D_{50}}{gh^2} + k_2 \frac{U^3}{gh\omega} + k_3 \frac{U^2 \Delta h}{gh\tilde{h}} \tag{7}$$

Replacing $S_1 + S_2 + S_3$ with k_4, Equation (7) becomes

$$S_c = k_1 \frac{U^2 D_{50}}{gh^2} + k_2 \frac{U^3}{gh\omega} + k_3 \frac{U^2 \Delta h}{gh\tilde{h}} + k_4 \tag{8}$$

The coefficients are determined using the least-square method (Ni et al. 2014). The objective function reads

$$f = \sum_{i=1}^{n} (k_1 \frac{U_i^2 D_{50i}}{g h_i^2} + k_2 \frac{U_i^3}{g h_i \omega_i} + k_3 \frac{U_i^2 \Delta h_i}{g h_i \tilde{h}_i} + k_4 - S_i)^2 \quad (9)$$

where n is the total number of data sets included in the analysis, and subscript i refers to the corresponding parameters of the i^{th} data set.

The following conditions are satisfied if the objective function reaches the minimum:

$$\frac{\partial f}{\partial k_1} = 0 \Rightarrow 2 \sum_{i=1}^{n} \frac{U_i^2 D_{50i}}{g h_i^2} (k_1 \frac{U_i^2 D_{50i}}{g h_i^2} + k_2 \frac{U_i^3}{g h_i \omega_i} + k_3 \frac{U_i^2 \Delta h_i}{g h_i \tilde{h}_i} + k_4 - S_i) = 0 \quad (10)$$

$$\frac{\partial f}{\partial k_2} = 0 \Rightarrow 2 \sum_{i=1}^{n} \frac{U_i^3}{g h_i \omega_i} (k_1 \frac{U_i^2 D_{50i}}{g h_i^2} + k_2 \frac{U_i^3}{g h_i \omega_i} + k_3 \frac{U_i^2 \Delta h_i}{g h_i \tilde{h}_i} + k_4 - S_i) = 0 \quad (11)$$

$$\frac{\partial f}{\partial k_3} = 0 \Rightarrow 2 \sum_{i=1}^{n} \frac{U_i^2 \Delta h_i}{g h_i \tilde{h}_i} (k_1 \frac{U_i^2 D_{50i}}{g h_i^2} + k_2 \frac{U_i^3}{g h_i \omega_i} + k_3 \frac{U_i^2 \Delta h_i}{g h_i \tilde{h}_i} + k_4 - S_i) = 0 \quad (12)$$

$$\frac{\partial f}{\partial k_4} = 0 \Rightarrow 2 \sum_{i=1}^{n} (k_1 \frac{U_i^2 D_{50i}}{g h_i^2} + k_2 \frac{U_i^3}{g h_i \omega_i} + k_3 \frac{U_i^2 \Delta h_i}{g h_i \tilde{h}_i} + k_4 - S_i) = 0 \quad (13)$$

A multivariate linear regression analysis is usually made to estimate k_1, k_2, k_3 and k_4.

3 Study area with data collection

The study area is in Southeast China. The water system includes a confluence called Sanjiangkou. Upstream of it, the two merging rivers are Fenghua and Yao; downstream it is the Yong River flowing into the Pacific Ocean (Figure 1). The Yong river length is ~26 km from the confluence to the river mouth. The area is significantly affected by the interplay between the river run-off (fresh water flow) and tidal currents, experiencing semi-diurnal tides (two nearly equal high and low tides each day) and belonging to the category of incomplete standing waves. The bed load in the area is negligibly small in quantity and the suspended load dominates, which is a common feature of many fluvial rivers.

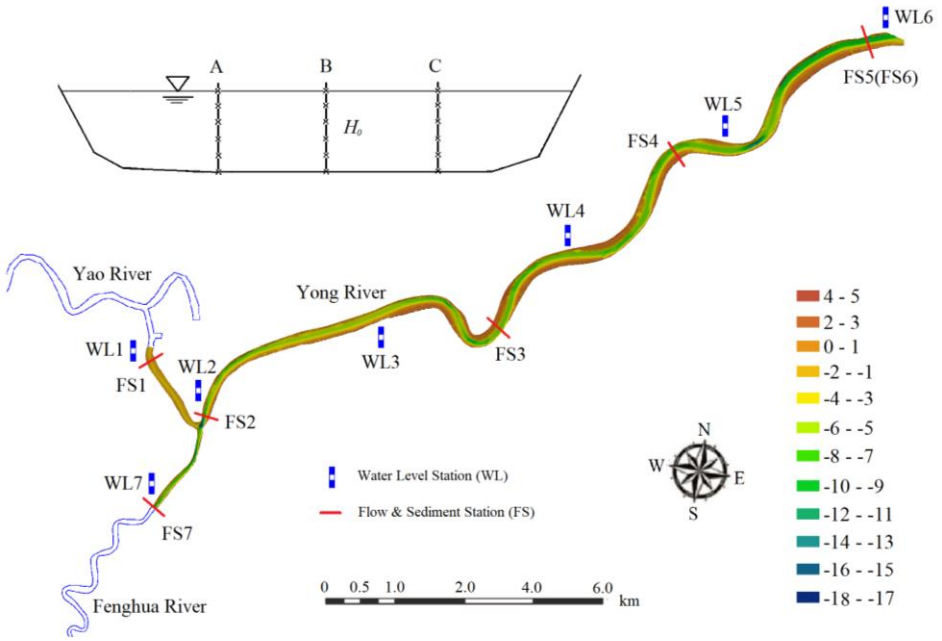

Figure 1. Hydrological stations of water levels (WL) and flow & sediment (FS) of the water system, with a cross-sectional sketch of measurement points.

Fenghua is 90–180 m in width and its average bed slope is 0.81%. The annual averaged runoff is 53.6 m^3/s; the annual sediment discharge is 4.35×10^4 ton (Chen et al. 2013). Yao is 180–230 m wide. Its daily runoff, as well as the sediment transport, is controlled by the sluice gates located 3.3 km upstream of the confluence. The annual sediment inflow to the study area is comparatively small. Yong runs roughly in the West-East direction, with a 150–250 m normal width. Its average river-bed slope is 0.117%; the annual mean runoff is ~92 m^3/s (Chen et al. 2013).

In the wet seasons, the peak discharge of the run-off and tides occurs normally during the 2nd half of June, amounting to ~1800 m^3/s. In the dry seasons, the peak occurs during the 1st half of January, equal to ~1100 m^3/s (Wang et al. 2015). The field stations for water levels (WL) and flow & sediment (FS) are also marked in Figure 1. At the river mouth, e.g., at WL6, the annual mean tidal range is 1.91 m; the flood and ebb durations are approximately the same, ~6 hrs. From the river mouth, the tidal asymmetry aggregates up the river. In the confluence, the ebb duration is 40 min longer than the flood duration. At WL7, the duration difference becomes 60 min. On Yao, the sluice gates stop the tidal currents to propagate further upstream. As for the location of the upstream limit of current reversals along Fenghua, the tides affect a reach of approximately 15 km upstream of WL7/FS7. The sediment in the area is mainly from the coastal area and is carried by the tides.

To record the tidal hydrological data, field surveys were carried out for the study area during the period June 2015 and January 2016. The data include water stage, flow velocity, flow discharge, sediment concentration and grain-size distribution, etc. The water levels were monitored at seven cross-sections (WL1–WL7), five of which were along Yong. To measure flow velocity and suspended sediment, seven cross-sections (FS1–FS7) were selected (Figure 1). FS5 and FS6 are a few meters apart from each other and are treated as the same section. At each cross-section, three plumb lines were arranged. Along each line, the sampling was made at six depths from the water surface, i.e., $h = 0$, $0.2H_0$, $0.4H_0$, $0.6H_0$, $0.8H_0$ and $1.0H_0$, where H_0 (m) is the water depth along each line. All the data were recorded at one-hour intervals.

For each station, either WL or FS, the time-series of data were analyzed. For each measurement interval, the time-averaged value was first obtained for each plumb line. The cross-sectionally averaged value was then achieved by the weighted average method.

4 Results

The measured data cover one wet season (the 2nd half of June 2015) and one dry season (the 1st half of January 2016). Due to difficulties in sediment measurements, data for only two typical tidal periods are available for each season, i.e. the spring tide (ST) and neap tide (NT). They are selected for the analysis.

Figure 2 shows the wet-season time-series of water levels Z (m) at the river mouth (WL6) and two upstream locations (WL1 & WL7). The ST occurs between 10:00 June 17 and 16:00 June 18, totaling 30 hrs. The NT occurs during a 31-hour period between 15:00 June 24 and 22:00 June 25 the in the same month. Based on the field data of the wet season, the coefficients of the formula are obtained. The data of the dry season are used for its verification.

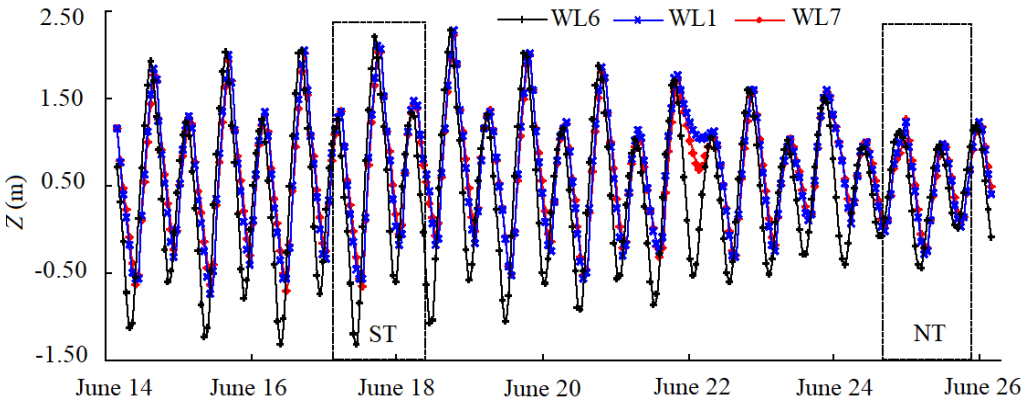

Figure 2. Time-series of Z at WL6, WL1 and WL7 in the wet season 2015

To investigate the spatial-periodical changes of the governing factors that affect the SCC, Table 1 summarizes the parameter ranges at FS1–FS7 during the ST and NT from the wet season. The following features are observed. S denotes the averaged sediment concentration in a cross-section.

Table 1. Parameter ranges during the ST and NT in the wet season (the 2nd half of June 2015)

Station	Tide	U (m/s)	h (m)	D_{50} (mm)	ω (mm/s)	Δh (m)	$\tilde{h}$ (m)	S (kg/m^3)
FS1	ST	0.04–0.47	1.50–4.40	0.003–0.007	0.35–0.49	−0.60–0.63	1.66–2.63	0.14–0.62
	NT	0.02–0.21	1.90–3.40	0.005–0.011	0.31–0.44	−0.30–0.30	0.93–1.48	0.03–0.10
FS2	ST	0.08–0.90	6.57–9.47	0.006–0.008	0.47–0.52	−0.60–0.90	1.46–2.90	0.28–1.23
	NT	0.11–0.69	6.97–8.47	0.005–0.009	0.41–0.49	−0.30–0.30	0.93–1.50	0.03–0.18
FS3	ST	0.07–1.01	6.20–9.00	0.006–0.009	1.55–1.66	−0.60–0.70	1.68–2.97	0.28–3.15
	NT	0.13–0.72	6.50–7.90	0.005–0.012	0.36–0.56	−0.37–0.30	0.93–1.47	0.12–0.32
FS4	ST	0.23–1.25	5.07–8.57	0.007–0.009	0.72–3.43	−0.70–0.90	1.98–3.51	0.59–4.48
	NT	0.15–0.98	5.97–7.37	0.004–0.009	0.54–2.46	−0.43–0.40	1.06–1.59	0.11–0.64
FS5 (FS6)	ST	0.33–1.30	6.67–10.17	0.007–0.009	1.32–2.02	−0.60–0.87	1.93–3.53	0.64–2.95
	NT	0.15–0.97	7.57–8.97	0.005–0.008	0.53–0.77	−0.80–0.77	1.02–1.56	0.11–0.96
FS7	ST	0.05–1.01	5.83–8.53	0.008–0.010	0.45–0.51	−0.50–0.80	1.48–2.70	0.37–1.54
	NT	0.10–0.84	6.33–7.77	0.006–0.013	0.41–0.48	−0.30–0.30	0.81–1.46	0.07–0.26

(1) During the ST, the range of U is 0.04−1.30 m/s; during the NT, it is 0.02−0.98 m/s. The h and Δh ranges during the ST are both larger than those during the NT. The $\tilde{h}$ range for the former is almost twice the value for the latter. This implies that the ST is comparatively strong.

(2) The D_{50} values vary between 0.003–0.010 mm during the ST; it is between 0.004–0.013 mm for the NT. The D_{50} values of the latter are slightly larger.

(3) S exhibits an increase from FS5 (FS6) to FS4; it then decreases up the river. The maximum S value on Yong occurs at FS4. For a given location, the ST shows higher S values than the NT. This indicates that the former governs the transport of the suspended sediment from the coastal area.

(4) At FS4 and FS5 (FS6), ω is larger than at the other stations. It implies that the flocculation effect of the suspended load is more intense at the estuary, which accelerates ω. During the ST, ω is larger than during the NT. This also illustrates that ST not only dominates the sediment transport but also increases the sediment collision and flocculation.

With the 30 + 31 = 61 temporal data sets at each cross-section, multivariate linear regression analysis is made in combination the least square method. Each set is cross-sectionally averaged. The resulting coefficients are: $k_1 = 0.026$, $k_2 = 0.019$, $k_3 = 0.013$ and $k_4 = 1.025$

Then the SCC formula takes the form

$$S_c = 0.026\frac{U^2 D_{50}}{gh^2} + 0.019\frac{U^3}{gh\omega} + 0.013\frac{U^2\Delta h}{gh\tilde{h}} + 1.025 \qquad (14)$$

which is rewritten as

$$S_c = \mathsf{F}^2 \left(0.026\frac{D_{50}}{h} + 0.019\frac{U}{\omega} + 0.013\frac{\Delta h}{\tilde{h}}\right) + 1.025 \qquad (15)$$

where $\mathsf{F} = U/(gh)^{0.5}$, the Froude number. Obviously, it considers flow turbulence, sediment property and tidal effects. In a tidal environment, the tides stir the sediment in water and modify its peak duration and transport. Field measurements show that the flow velocity and sediment concentration within a tidal period are always out of phase with each other (Xie et al. 2018, 2019). The peak-tide method (Sun, 2017) and the half-tide method (Pan et al. 2013) don't include the lag effect between the sediment and flow. The proposed whole-tide method overcomes this and is therefore preferable.

The reliability of the derived formula is verified with the aid of the 30 + 32 = 62 sets of the hourly measured data from the dry season. Figure 3 presents the corresponding Z values. The ST occurs between 16:00 January 9 and 22:00 January 10 (30 hrs) and the NT between 9:00 January 3 and 17:00 January 4 (32 hrs).

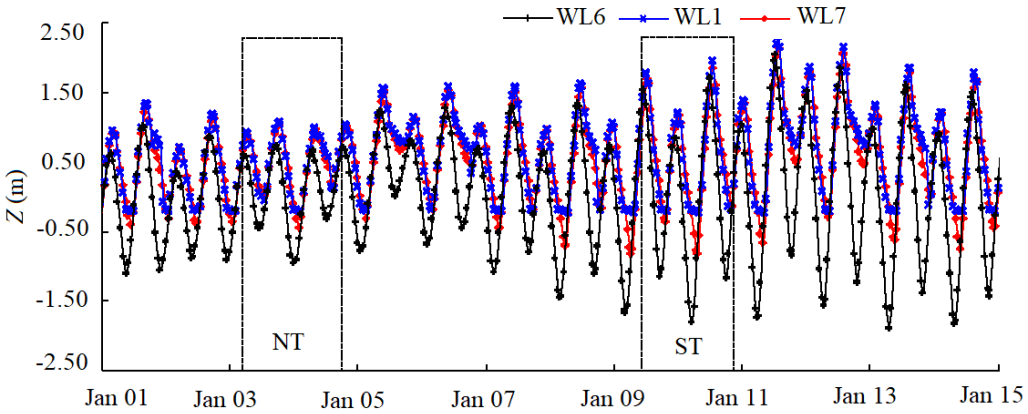

Figure 3. Time-series of Z at WL6, WL1 and WL7 in the dry season 2016

Table 2 shows the parameter ranges during the ST and NT in the dry season. Compared to the wet season, the spatial-periodical features of the flow and sediment are similar. However, U, ω and S are smaller in magnitude, implying that both the run-off and the tides are weaker.

Table 2. Parameter ranges during the ST and NT in the dry season (the 1st half of January 2016)

Station	Tide	U (m/s)	h (m)	D_{50} (mm)	ω (mm/s)	Δh (m)	$\tilde{h}$ (m)	S (kg/m^3)
FS1	ST	0.02–0.43	1.60–4.70	0.003–0.006	0.33–0.45	−0.43–0.63	1.41–2.18	0.07–0.30
	NT	0.02–0.19	1.87–3.53	0.004–0.009	0.27–0.42	−0.35–0.37	0.87–1.30	0.03–0.08
FS2	ST	0.05–0.83	6.57–9.43	0.005–0.008	0.27–0.71	−0.50–0.70	1.69–2.80	0.10–0.66
	NT	0.04–0.69	7.03–8.53	0.005–0.007	0.31–0.65	−0.30–0.40	0.89–1.54	0.06–0.20
FS3	ST	0.20–1.10	3.47–6.07	0.005–0.008	1.23–1.35	−0.60–0.80	1.73–2.83	0.22–1.60
	NT	0.02–0.82	3.67–5.27	0.004–0.005	0.36–0.54	−0.40–0.30	0.95–1.55	0.07–0.35
FS4	ST	0.08–1.35	5.20–8.70	0.006–0.007	1.53–2.66	−0.40–0.80	2.03–3.52	0.59–2.37
	NT	0.07–0.79	6.00–7.70	0.004–0.006	0.48–2.14	−0.40–0.40	0.98–1.71	0.05–0.30
FS5 (FS6)	ST	0.08–1.28	7.37–10.87	0.006–0.007	1.02–1.85	−0.60–0.80	2.89–3.52	0.52–1.33
	NT	0.15–0.79	8.27–9.87	0.005–0.007	0.48–0.63	−0.40–0.80	0.97–1.69	0.04–0.61
FS7	ST	0.09–0.91	5.53–8.13	0.007–0.010	0.38–0.48	−0.50–0.70	1.53–2.66	0.08–0.59
	NT	0.05–0.72	5.83–7.33	0.005–0.007	0.36–0.45	−0.30–0.30	0.81–1.52	0.07–0.20

Figure 4 shows the comparison between the prediction and measurements. The horizontal and vertical axes refer to the measured (S) and predicted values (S_c), respectively. Suppose that the total number data used for the ST or NT analysis is n. Within a deviation band $\leq \pm e$ from the SCC formula, the total data number is denoted as n_e. Let P (%) = n_e/n, representing the percentage of data within the interval.

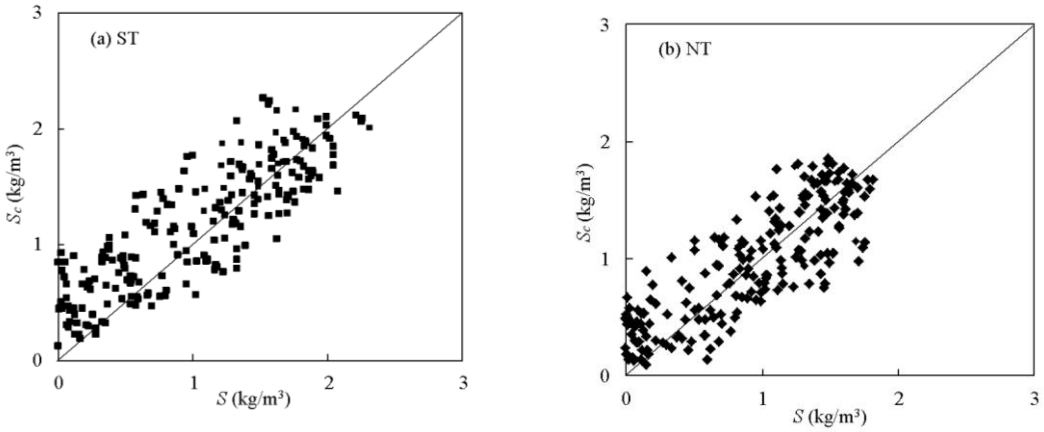

Figure 4. Comparison of S_c and S during ST and NT in the dry season (the 1st half of January 2016)

At each station in the dry season, the accuracy of prediction is further illustrated in Table 3, with e = 5% and 10%. Even the overall error is given for each station. This indicates that the derived SCC formula reasonably reproduces the data in the tidal river.

Table 3. Accuracy of prediction applied to the tides during the dry season.

Period	Station	P (%)		Overall error
		e = 5%	e = 10%	
ST	FS1	83	90	12.78
	FS2	85	88	11.25
	FS3	88	92	8.85
	FS4	89	91	8.56
	FS5(FS6)	85	91	10.32
	FS7	82	90	14.55
NT	FS1	82	89	15.78
	FS2	84	87	14.38
	FS3	87	90	9.56
	FS4	88	91	9.23
	FS5(FS6)	85	89	12.75
	FS7	83	87	16.82

5 Conclusions

In a river subjected to the interaction of run-off and tidal currents, the carrying capacity of suspended load is dependent on a number of factors, exhibiting complex features in both time and space. With the field measurements in the background, the study deals with the typical features of such a river by means of theoretical analysis.

Based on the perturbation theory, combined with dimensional analysis, multivariate linear analysis and least squares method, an approach to estimate the sediment carrying capacity is presented for a tidal river and a capacity formula is established. The procedure includes such factors as flow turbulence intensity (U^2/gh), gravity action (U/ω), relative roughness (D_{50}/h), median grain size (D_{50}) and tidal effect ($\Delta h/\tilde{h}$). It is an improvement compared with previous studies considering fewer parameters. The derived formula has relatively good prediction accuracy. It is advisable to take into consideration the median grain size and tidal effects in determination of the sediment carrying capacity.

Acknowledgments

The first author is funded by a four-year Ph.D. scholarship from the Chinese Scholarship Council (CSC) and the Swedish STandUp for Energy project. The field measurement data are from the Hydrology and Water Resources Survey Bureau of the Lower Yangtze River. The authors are all members of the 111 Project at Hohai University (Discipline Innovation and Research Base on River

Network Hydrodynamics System and Safety, Grant No. B17015), funded by the Ministry of Education and State Administration of Foreign Experts Affairs, China.

References

[1] Chen, J., Tang, H.W., Xiao, Y., and Ji, M. (2013). "Hydrodynamic characteristics and sediment transport of a tidal river under influence of wading engineering groups". China Ocean Engineering, 27(6), 829–842.

[2] Engelund, F., and Hansen, E. (1967). "Comparison between similarity theory and regime formulae". Basic Research-Progress Report 13, Hydraulic Laboratory, Technical University of Denmark.

[3] Milhous, R.T. "Climate change and changes in the sediment transport capacity in the Colorado Plateau, USA". In the 7th IAHS Scientific Assembly, Sediment budgets 2, April, 2005, Foz do Iguacu, Brazil.

[4] Ni, Z.H., Zeng, Q., and Wu, L.C. (2014). "Determination of the sediment carrying capacity based on perturbation theory". The Scientific World journal, Article ID 240858.

[5] Sun, J. (2017). "Study on the movement characteristics of fine sediment in the Yong river estuary". Master thesis. Hohai University, Nanjing, China.

[6] Pan, C.H., Zeng, J., Tang, Z.W., and Shi, Y.B. (2013) "Research on the sediment characteristics and riverbed erosion and sedimentation in the Qiantang River estuary". Hydo-Science and Engineering (in Chinese), 1, 1–7.

[7] Wang, H., Sha, H., Lu, D., He, L., and Guo, K. (2015). "Hydrological and topographic survey of Ningbo Yongjiang sluice gates constructon (2nd phase)". Technical Report, Hydrology and Water Resources Survey Bureau of the Lower Yangtze River, China.

[8] Xie, Q.C., Yang, J., T. Lundström, S., and Dai, W.H. (2018). "Understanding morphodynamic changes of a tidal river confluence through field measurements and numerical modeling". Water, 10, 1424.

[9] Xie, Q.C., Yang, J., and T. Lundström, S. (2019). "Field studies and 3D modelling of morphodynamics in a meandering river reach dominated by tides and suspended load". Fluids, 4, 4010015.

[10] Yang, S.Q., Koh, S.C., Kim, I.S., and Song Y. (2007). "Sediment transport capacity: an improved Bagnold formula". International Journal of Sediment Research, 22(1), 27–38.

[11] Zhang, R.J. (1961). "River Mechanic". China Industry Press, Beijing, China.